Integrating annual radial growth analyses and carbon isotope discrimination to forecast early warning of beech forest dieback across the Italian Peninsula

Running head: Forecasting European beech mortality risk

PAULINA F. PUCHI[1,2*], DANIELA DALMONECH[1,3], ELIA VANGI[1], GIOVANNA BATTIPAGLIA[4], ROBERTO TOGNETTI[5] and ALESSIO COLLALTI[1,3]

[1]Forest Modelling Lab., Institute for Agriculture and Forestry Systems in the Mediterranean, National Research Council of Italy (CNR-ISAFOM), Via Madonna Alta 128, 06128 Perugia, Italy

[2]Institute of Bioeconomy, Italian National Research Council (CNR-IBE), Via Madonna del Piano 10, 50019 Sesto Fiorentino, Italy

[3]National Biodiversity Future Center (NBFC), 90133 Palermo, Italy

[4]Department of Environmental, Biological and Pharmaceutical Sciences and Technologies, University of Campania 'L. Vanvitelli', Caserta, Italy

[5]Department of Agricultural, Environmental, and Food Sciences, University of Molise, Via De Sanctis, 86100 Campobasso, Italy

[*]***Corresponding author***

ORCID ID: 0000-0001-5429-8605

e-mail: paulina.puchi@isafom.cnr.it

Keywords: Growth decline, climate change, basal area increment, SPEI, VPD, dendrochronology, water use efficiency, carbon stable isotopes, autocorrelation.

Paper type: Primary Research

ABSTRACT

Tree mortality and forest dieback episodes are increasing due to drought and heat stress. However, a comprehensive understanding of the mechanisms enabling trees to cope with droughts remains lacking. Here, we employed a multi-proxy method utilizing tree-ring width, basal area increment (BAI) trends, and $\delta^{13}C$-derived intrinsic water-use-efficiency ($_{i}WUE$) to unravel beech resilience against drought stress. We selected four sites spanning the latitudinal gradient and beech distribution in northern (Trentino-TRE), central (Lazio-LAZ), southern (Campania-CAM) and southernmost Italy (Calabria-CAL) with different climate conditions and soil water availability.

First-order autocorrelation (AR1) analysis was performed to detect early warning signals for potential tree dieback risks during extreme drought events. Results revealed a negative correlation between vapour pressure deficit (VPD) and BAI, especially at southern latitudes. GAMM analysis showed a negative trend in BAI across most sites, stronger at the TRE site following the 2003 drought event. During this event, $\delta^{13}C$ and $_{i}WUE$ increased with rising VPD, indicative of conservative water-use (lower stomatal conductance) and contributing to the decline in BAI. Conversely, CAM exhibited a steady increase in BAI and $_{i}WUE$, likely influenced by rising atmospheric CO_2 and water availability. LAZ site exhibited a decrease in $\delta^{13}C$, attributed to greater soil water holding capacity, enabling it to sustain higher transpiration rates. Conversely, southern sites presented higher $_{i}WUE$, likely as high VPD initially reduces stomatal conductance but not the net assimilation rate, resulting in increased $_{i}WUE$. Nevertheless, almost all sites exhibited a co-occurrence of increase in AR1 (except for CAM) and standard deviation, suggesting a reduction of resilience to future extreme events.

Overall, multi-proxy, retrospective quantifications of BAI, $_{i}WUE$ and resilience provide a robust and complementary tool for differentiating water-use strategies and predicting tree growth decline and dieback, as well as identifying those that have the potential to survive in warmer and drier future conditions.

1 INTRODUCTION

Forest ecosystems are facing significant challenges due to anthropogenic climate change (Allen et al., 2010; McDowell et al., 2020). The combination of reduced water availability and rising temperatures directly impacts the process of photosynthetic carbon assimilation, thereby reducing forest carbon sequestration (Keenan, 2015; Zuidema et al., 2018). This could potentially lead to negative feedback on carbon balance (Pan et al., 2011). Furthermore, hotter droughts have caused substantial alterations in forest structure and function, affecting tree growth performance and triggering episodes of dieback and tree mortality (Allen et al., 2015; Anderegg et al., 2016: Puchi et al., 2021). In addition, climatic models predict that the frequency, duration, and intensity of extreme droughts will increase in the future (IPCC 2021), so it is crucial to a better understanding of how forests are going to cope with these extreme climatic conditions (Brodribb et al., 2020).

Despite the importance of identifying suitable tree species and future management practices in response to climate change, our understanding of species-specific physiological responses and site- and species-specific vulnerabilities to drought-induced tree mortality during extreme droughts remains incomplete (Allen et al., 2015; Trugman et al., 2021; De Marco et al., 2022). This gap is especially critical for European beech (*Fagus sylvatica* L.), one of the most distributed, ecologically and economically significant tree species in Europe (Fang and Lechowicz 2006). This species comprises 17% of all broadleaf tree stands in Italy (Gasparini et al., 2022) and is one the most affected by extreme events occurring during the initial vegetative phase across the Italian peninsula (D'Andrea, et al., 2020; Martinez del Castillo et al., 2022; Tonelli et al., 2023).

Given the anticipated that climate change will exert a significant influence on both regional and local drought patterns in the Mediterranean region (Adams et al., 2017; Sangüesa-Barreda et al., 2019). In particular, mountain-Mediterranean beech forests would face increased vulnerability due to their location in the southernmost distribution of this species' range (Noce et al., 2016, 2017; Leuschner

2020; D'Andrea et al., 2021). Consequently, predicting resilience and adaptation across its distribution has become a prioritized goal.

Recent studies have shown that prolonged heat and drought events can have detrimental effects on both hydraulic function and carbon use in trees (McDowell et al., 2008; Anderegg et al., 2013). Understanding these physiological mechanisms is crucial for comprehending how trees respond to drought, as they directly influence water use regulation. For instance, isohydric species adopt a conservative behaviour by closing stomata to minimize water loss, thereby reducing photosynthetic activity, and increasing the risk of carbon starvation (Timofeeva et al., 2017). On the other hand, anisohydric species adopt an opportunistic behaviour, exhibiting higher transpiration rates even when soil moisture is low, leading to an elevated risk of hydraulic failure (McDowell et al., 2008; Petrucco et al., 2017).

Currently, there is contrasting information regarding how European beech forests respond to heat and drought events (Leuschner, 2020; D'Andrea et al., 2021). Most studies on young beech stands have suggested a conservative response during droughts (Leuschner, 2020; Walthert et al., 2021; Martinez del Castillo et al., 2022). However, in a few studies, adult trees have conversely displayed opportunistic behaviour (Leuschner, 2020). Therefore, it is crucial to exploit better the plasticity of this species in the water use strategies to determine the trajectories of species distribution and its resilience to a warming and drier climate (Gessler et al., 2020; Walthert et al., 2021).

Long-term changes in intrinsic water use efficiency ($_{i}$WUE), i.e. the cost of fixing carbon per unit of water loss (Seibt et al., 2008; Gagen et al., 2022), can be assessed by measuring carbon isotope composition in tree rings ($\delta^{13}C$). Tree-ring $\delta^{13}C$ is equivalent to the ratio between photosynthesis (A) and stomatal conductance (g_s) and this can vary, since both affect the ratio between CO_2 partial pressure in leaf intercellular space and in the atmosphere (Farquhar et al., 1982; Battipaglia and Cherubini, 2022). Variations in $_{i}$WUE, within and across tree species, have revealed a continuous ecophysiological gradient of plant water-use strategies ranging from "profligate/opportunistic" (low

$_i$WUE) to those considered "conservative" (high $_i$WUE) (Moreno-Gutiérrez et al., 2012). For instance, studies in tree rings have shown that the increase of $_i$WUE did not enhance tree growth (Peñuelas et al., 2011), however, others showed the opposite effect or both (Peñuelas et al., 2008; Tognetti et al., 2014; Walker et al., 2021). These indicators of hydraulic strategies and carbon discrimination provide valuable insights into the long-term impacts of climate change on forest health and the risk of tree mortality (Gessler et al., 2018; Cherubini et al., 2021; Puchi et al., 2021).

On the other hand, recent studies have provided evidence that one of the primary mortality risk indicators in forests is growth reduction also occurring many decades before visible symptoms of decline, such as leaf discolouration, increased defoliation, and branch dieback (Camarero et al., 2015; Cailleret et al., 2016; 2019; DeSoto et al., 2020). Similarly, another proxy indicator of loss of resilience and thus increasing tree mortality risk is the autocorrelation, better called 'early warning signal' (EWS), which has been proposed to detect a critical transition in long-term time series after a perturbation, causing a critical slowing down of the capacity of recovery (Dakos et al., 2012a; Gessler et al., 2020; Forzieri et al., 2021). EWS can be highlighted as increasing autocorrelation and variance in tree growth, indicating loss of resilience and stability (Dakos et al., 2012a; 2012b). These changes have been observed in conifers; however, angiosperms did not show changes in these indicators, and this could be due to their capacity to recover after a stress-induced growth decline (Camarero et al., 2015; Cailleret et al., 2019). These findings highlight the importance of early monitoring in understanding forest resilience and adaptation to climate change.

This study aimed to assess the forest vitality of beech in response to drought stress by examining historical and recent growth patterns across the Italian peninsula, with a particular emphasis on water use strategies (conservative vs. opportunistic) at long-time scales. Secondly, we tested early warning signals of potential tree dieback by analyzing autocorrelation and variability patterns, as indicators of stand resilience and stability to future extreme events.

We hypothesized that beech populations in the southernmost distribution exhibit conservative behaviour as an acclimation strategy. This behaviour is characterized by $_i$WUE being more responsive to VPD than those in the northern regions, reflecting a reduction in stomatal conductance to maintain a minimum midday water potential, and also a decline in intercellular CO_2 concentration, but a more slowly decrease in photosynthetic rate. Although a drought-driven decline in photosynthetic rate may also occur, non-stomatal limitation was expected in populations with more opportunistic behaviour. Additionally, we expected to find varying degrees of growth reduction as an early warning signal of tree mortality risk across different sites, with the strongest signals in response to severe drought events.

2 MATERIALS AND METHODS

2.1 Study sites and climate

Analyses were conducted at four sites along a ~900 km latitudinal transect in pure European beech forests across the Italian Peninsula (Figure 1, Table 1). The sites were Trentino-Alto Adige (hereafter abbreviated as 'TRE'), Lazio (hereafter abbreviated as 'LAZ'), Campania (hereafter abbreviated as 'CAM') and Calabria (hereafter abbreviated as 'CAL'). All the stands analyzed had not been managed since the last 20-30 years.

The selection of the sites allowed the comparison of moisture availability across the Italian Peninsula (Figure 1), using the Climate Moisture Index (CMI) calculation method explained in section 2.6. These sites differ along the latitudinal transect regarding both climatic conditions and soil types. From north to south, the mean annual temperature ranges from 9 to 14.1 °C, with the mean annual precipitation varying from 1003 to 825 mm, based on the E-OBS dataset (as explained in section 2.4; Figure S1)

150 The soil types from north to south are Andisols, Luvisols, and Inceptisols. Additionally, by examining
151 soil texture data, we inferred variations in soil water holding capacity (SWHC) among these sites
152 (Table S1, Hengl and Nauman, 2018). Specifically, we inferred that the SWHC in TRE is relatively
153 low, whereas LAZ exhibited a high SWHC. CAM also showed a high SWHC, while CAL presented
154 a moderate SWHC (Kutílek and Nielsen, 1994).

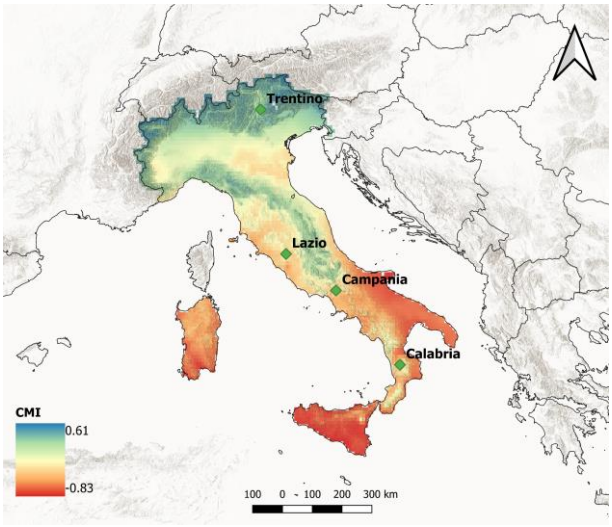

155

156 **Figure 1** a) Map displaying the Climate Moisture Index (CMI = Precipitation / Potential
157 EvapoTranspiration) across the Italian Peninsula, indicating humid and dry climate zones through
158 positive (blue) and negative (red) CMI values, respectively. The index was calculated for the
159 growing season (May-October) from 1965 to 2014. Green dots indicate the location of the four
160 study sites where dendrochronological samples were extracted.

161

162 **Table 1.** Geographical and mean annual climate characteristics for the four sites.

Site	Latitude (N)	Longitude (W)	Elevation (m a.s.l.)	Mean minimum annual temperature (°C)	Mean annual temperature (°C)	Mean maximum annual temperature (°C)	Annual precipitation (mm)	Reference
TRE	46°12'	11°16'	1276	3.8	9.0	13.9	929	TRW data Versace et al., 2020

LAZ	42°24'	12°12'	1000	8.9	14.3	19.5	829	Battipaglia et al., unpublished
CAM	41°24'	14°20'	1140	6.3	9.8	13.1	825	Battipaglia et al., unpublished
CAL	39°19'	16°23'	1601	5.8	11	16	1003	Battipaglia et al., unpublished

2.2 Field sampling and processing dendrochronological data

During the period 2014-2018, a total of 174 beech trees were sampled at 1.3 m from the ground using a 5 mm increment borer (Table S2). In the laboratory, wood cores were air/dried and polished with sandpaper of successively increasing grains to visualize the ring boundaries. Ring widths were measured to a precision of 0.01 mm using the TSAP measuring device (Rinntech). Tree-ring (TRW) series were then visually cross-dated using standard dendrochronological methods (Stokes and Smiley, 1968) and checked for dating accuracy and measurement errors with the COFECHA program (Holmes, 1983).

Later, tree growth measurements were converted to basal area increment based (BAI) based on the distance between the outermost measured ring (pith) and the last ring of the tree (i.e., the ring next to the bark), using the following formula:

$$BAI = \pi (R^2_t - R^2_{t-1}), \quad (1)$$

where R_t the tree's radius at the end of the annual increment, and R_{t-1} is the tree's radius at the beginning of the annual increment. This method assumes a circular cross-section, and the mean BAI of defined periods can be compared over time, as it is not affected by biological trends (Biondi and Qeadan, 2008a; 2008b) and it is more tightly related to stem biomass compared to TRW. We worked with mean non-standardized BAI values to preserve the long-term cumulative effects of climate on tree growth (Tognetti et al., 2014). All analyses were restricted to the period covered by the youngest

trees (at LAZ), i.e. from 1965 until 2014 (Table S2). All computations were performed using the R-package 'dplR' (Bunn, 2008; Bunn et al., 2021; R Core Team, 2022).

2.3 Water-use efficiency from carbon isotope discrimination

To compare long-term changes in $_i$WUE among beech trees across the Italian Peninsula, we measured $^{13}C/^{12}C$ isotope ratios in the TRW. Ten samples per each stand presenting the best cross-dating (GLK > 0.70) with the corresponding average chronology, were selected for stable isotope analyses (Battipaglia et al., 2017) and they were annually dissected using a razor blade under a binocular microscope for the period 1965-2014.

Wood samples were milled to a fine powder (ZM 1000; Retsch), weighed 0.05-0.06 mg of wood for carbon isotope analyses and encapsulated in tin capsules.

The isotope composition was measured at the IRMS laboratory of the University of Campania "Luigi Vanvitelli" by using mass spectrometry with continuous flow isotope ratio (Delta V plus Thermo electron Corporation). The standard deviation for repeated analysis of an internal standard (commercial cellulose) was better than 0.1‰ for carbon. The $\delta^{13}C$ series were corrected for the fossil fuel combustion effect for anthropogenic changes in the atmospheric $\delta^{13}C$ composition ($\delta^{13}C_{atm}$) (Francey et al., 1999; McCarroll and Loader, 2004).

Isotopic discrimination between the carbon of atmospheric CO_2 and wood carbon to determine $_i$WUE can be calculated starting from the $\delta^{13}C$ of the plant material ($\delta^{13}C_{tree}$), which is related to atmospheric $\delta^{13}C$ ($\delta^{13}C_{atm}$) and the ratio c_i/c_a, according to Farquhar and Richards (1984) and Farquhar et al. (1982):

$$\delta^{13}C_{tree} = \delta^{13}C_{atm} - a - [(b - a)\, c_i] / c_a, \quad (2)$$

where a is the fractionation factor due to $^{13}CO_2$ diffusion through stomata (4.4‰), and b is the fractionation factor due to Rubisco enzyme during the process of carboxylation (27‰) (McCarroll and Loader, 2004). Therefore, we can calculate c_i by using the formula:

$$c_i = c_a(\delta^{13}C_{atm} - \delta^{13}C_{tree} - a) / (b - a) . \quad (3)$$

Finally, the $_i$WUE can be calculated as follows:

$$_iWUE = (c_a b - \delta^{13}C_{atm} + \delta^{13}C_{tree}) / 1.6 (b - a). \quad (4)$$

However, the $_i$WUE should not be considered equivalent to instantaneous WUE at leaf level, which is the ratio of assimilation to stomatal conductance and considers the atmospheric water demand (Pacheco et al., 2020; Seibt et al., 2008). Thus, the equation used is the "simple" form of isotopic discrimination that does not include effects due to mesophyll conductance and photorespiration, which were unavailable for the study species.

We used $\delta^{13}C_{atm}$ values from Belmecheri and Lavergne (2020). We obtained the atmospheric concentration of CO_2 from the Mauna Loa station data (http://www.esrl.noaa.gov/).

2.4 E-OBS daily climate data, CMI and SPEI calculation

Daily climate data for precipitation (P), minimum (T_{min}), mean (T_{mean}), and maximum (T_{max}) temperature, as well as relative humidity (RH), were extracted from the E-OBS dataset on a regular 0.1-degree grid (Table 1). The data were obtained as netCDF files from (http://surfobs.climate.copernicus.eu/dataaccess/access_eobs.php). Using the RH and temperature data, the vapour pressure deficit (VPD) in hPa was calculated based on the Tetens formula (Tetens 1930).

The Climate Moisture Index (CMI, Willmott and Feddema, 1992) represents the relationship between plant water demand and available precipitation. The CMI indicator ranges from –1 to +1, with wet climates showing positive CMI and dry climates negative CMI. CMI was calculated as follows:

$$CMI = P/PET \quad (5)$$

Where P is the precipitation, and PET is the potential evapotranspiration. Specifically, CMI = (P/PET) –1 when P<PET and CMI = 1–(PET/P) when P>PET, to recast the limit to –1<CMI<1.

PET can be calculated through the Hargreaves equation (Hargreaves, 1985), modified by Allen (1993):

$$PET = 0.0029\ R_{solar\_rad}\ (T_{mean}+20)\ TR^{0.4} \quad (6)$$

Where R_{solar_rad} is the extraterrestrial solar radiation, T_{mean} in Celsius degree and TR is the temperature range (T_{max}–T_{min}).

CMI was calculated for the growing season (May-October) using the E-OBS v. 27.0 (https://surfobs.climate.copernicus.eu/dataaccess/access_eobs.php#datafiles) daily products (T_{min}, T_{max}, precipitation, and global solar radiation) at 0.1 deg spatial resolution and averaged over the period 1965-2014. E-OBS global solar radiation at the surface was converted to extra-terrestrial solar radiation with the 'envirem' R-package (Title and Bemmels, 2018).

Additionally, to quantify drought severity, we calculated the Standardized Precipitation-Evapotranspiration Index (SPEI), based on a statistical transformation of the climatic water balance, i.e. precipitation *minus* potential evapotranspiration (P-PET) (Vicente-Serrano et al., 2010). The multiscalar drought index was calculated at different time scales (from 1 to 24 months, Figure S2) for the period 1965-2014 (constrained to the youngest site LAZ) in R using the 'SPEI' package (Beguería et al., 2014; Beguería and Vicente-Serrano, 2017).

Later, to assess the relationships between climate and BAI and stable isotope for the period 1965–2014, we calculated Pearson's correlations between monthly P, T_{mean}, VPD, and SPEI (1-3-6-9-12-

18 and 24 months) series from previous $_{(t-1)}$ and current year $_{(t)}$, using monthly response function in the 'DendroTools' R-package (Jevšenak and Levanič, 2018).

2.5 Growth trends and climate response

We used Generalized Additive Mixed Models (GAMM) to study the long-term annual BAI and their responses to changing climatic conditions, particularly concerning water balance within the growing season (May-October) using SPEI indexes at the four study sites. We tested SPEI drought index at 1,3,6,9,12,18, and 24 months as the potential influence of drought on BAI. GAMM is a flexible semiparametric method that allows the simultaneous modelling of linear and nonlinear relationships between the response variable as a function of some explanatory variables (Wood, 2006) that allows the treatment of autocorrelation and repeated measures (Wood, 2006). The variables included in the model were the following:

$$BAI_i = s[year_i*(Site)]+s(age_i)+s(SPEI_i)+Z_iB_i+\varepsilon \quad (5)$$

Where the BAI_i of a $tree_i$ were modelled as a function of calendar year, individual tree age and SPEI per site. In addition, given that BAI represents multiple measurements performed in each tree, tree identity (Z_iB_i) is regarded as a random effect (Z_i and B_i indicate matrix variables and related coefficients). Thin plate regression splines (s) were used to represent all the smooth terms, with a degree of smoothing determined by internal cross-validation (Wood, 2006). We ranked all the potential models that could be generated using different explanatory variables and different levels of smoothing according to the Akaike Information Criterion (AIC). Finally, we chose the model with the lowest AIC (Burnham and Anderson, 2002). The time scale that best explained the variability in BAI was the 18-month SPEI (for the growing season May-October). The GAMMs were performed and fitted using the function 'gamm' in the 'mgcv' R-package (Wood, 2006).

2.6 Early warning signals of forest dieback

For assessing stand resilience for each site and each time series of BAI, we computed the autocorrelation at lag-1 (AC) and the standard deviation (SD) over the period 1965 to 2014 using a 15-year moving window (30% of the entire time series). These metrics are widely recognized indicators of changes in time series and proximity to critical transitions to new states (Dakos et al., 2012a; Camarero et al., 2015; Forzieri et al., 2022). The trend of AC and SD metrics over the considered temporal window was computed by means of the non-parametric Mann-Kendall Tau statistics. For each site, the significance of a positive (or negative) AC and SD trend was tested with a one-sided t-test. We employed the R-package 'early warnings' (Dakos et al., 2012b) to compute the selected metrics. All statistical analyses were conducted using the R-statistical software (R Development Core Team, 2022)

3 RESULTS

Climate trends and drought variability

Annual precipitation (P) has increased significantly at TRE and CAM sites ($p < 0.01$, Figure S2a), while LAZ showed a reduction in P trend during the period from 1965 to 2014 ($p < 0.05$, Figure S2a), and CAL did not present any trend in P pattern. Notably, T_{min} increased significantly in TRE, LAZ, and CAM ($p < 0.001$, Figure S2b), whereas in the southern site (CAL), T_{min} presented a pronounced decrease ($p < 0.01$, Figure S2b). Simultaneously, both T_{mean} and T_{max} exhibited a substantial and significant increase across all sites ($p < 0.01$, Figure S2c and S2d). Interestingly, only at the northernmost site (TRE), VPD increased drastically and significantly during the 2000s ($p < 0.001$, Figure S2e), while at the southernmost site (CAL) VPD showed the opposite pattern (Figure S2e, $p < 0.001$).

297 As for the P trend, the SPEI index showed an increase in water availability in recent years across
298 sites, although not significant, except for LAZ, which showed a negative trend ($p < 0.05$, Figure 2,
299 Figure S3). Notably, the SPEI-derived drought index showed the widespread impact of the 2003
300 drought across all sites, more evident at CAM (Figure 2, Figure S3).

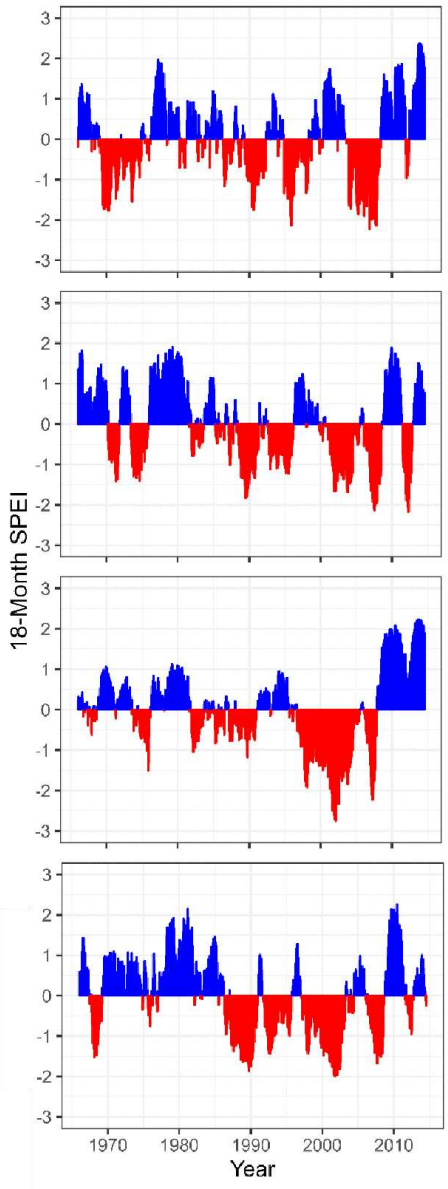

301

302 **Figure 2** Standardized 18-Month SPEI at the four study sites (TRE, LAZ, CAM, and CAL) for the
303 1965–2014 period. Negative (red) and positive (blue) values indicate drier and wetter conditions,
304 respectively.

305

306 **Long-*term growth trends of Fagus sylvatica across the Italian Peninsula***

307 Mean TRW, the highest and the lowest growth rates were observed in LAZ and CAM sites,
308 respectively with statistically significant differences. Conversely, TRE and CAL showed similar
309 growth rates values ($p < 0.05$, Table S3). The age distribution of tree populations exhibited notable
310 differences across the four sites, with LAZ featuring the youngest trees and CAM the oldest trees (p
311 < 0.05, Table S3).

312 BAI exhibited a significant decline, particularly pronounced in the relatively northern sites (TRE and
313 LAZ), following the drought of 2003 (Figure 3b). In contrast, CAM presented a steady increase in
314 BAI, while in CAL, BAI decreased after 2010 (Figure 3b).

315

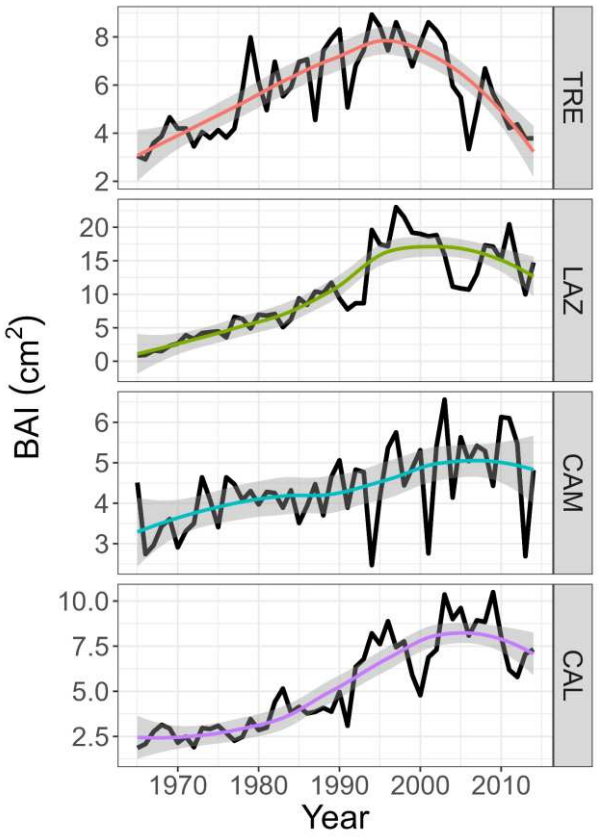

316

317 **Figure 3** Long-term growth of basal area increment (BAI) of the four sites along a latitudinal gradient
318 (north to south) for the period 1965–2014. Colour lines for each site indicate the linear model, shaded
319 areas represent 95 % confidence intervals.

320

321 **Growth response to climate variables**

322 Basal area increment exhibited significant relationships with climatic variables in all study sites
323 (Figure 4). Overall, BAI was positively correlated with monthly P and T_{mean} and, notably, strongly
324 negative correlations with VPD were evident from May to September. This negative VPD correlation
325 intensified toward the southern sites (Figure 4).

326 At TRE, BAI was positively correlated with monthly P from May to July, with a stronger effect when
327 considering P values in the previous year. Additionally, BAI correlated positively with May T_{mean} of
328 the current year, instead of showing weak negative correlations with VPD and SPEI (Figure 4).

329 LAZ showed a strong positive correlation between BAI and T_{mean} from March to November (previous
330 and current year). Conversely, strong negative correlations with VPD from May to September and
331 weak negative correlations with P and SPEI were found in August (Figure 4).

332 AT CAM, a positive response of BAI to P of July of the previous years, and a strong positive
333 correlation with T_{mean} during May to July, were observed, while a strong negative response to VPD
334 from March to September (more evident in the current year) was found.

335 At CAL, BAI showed strong positive correlations with October P and with T_{mean} from March to
336 August. In contrast, BAI displayed a strong negative correlation with VPD from March to September
337 (current and previous year). Similarly, negative scattered correlations with SPEI were observed
338 during summer at the southern sites (CAM and CAL, Figure 4).

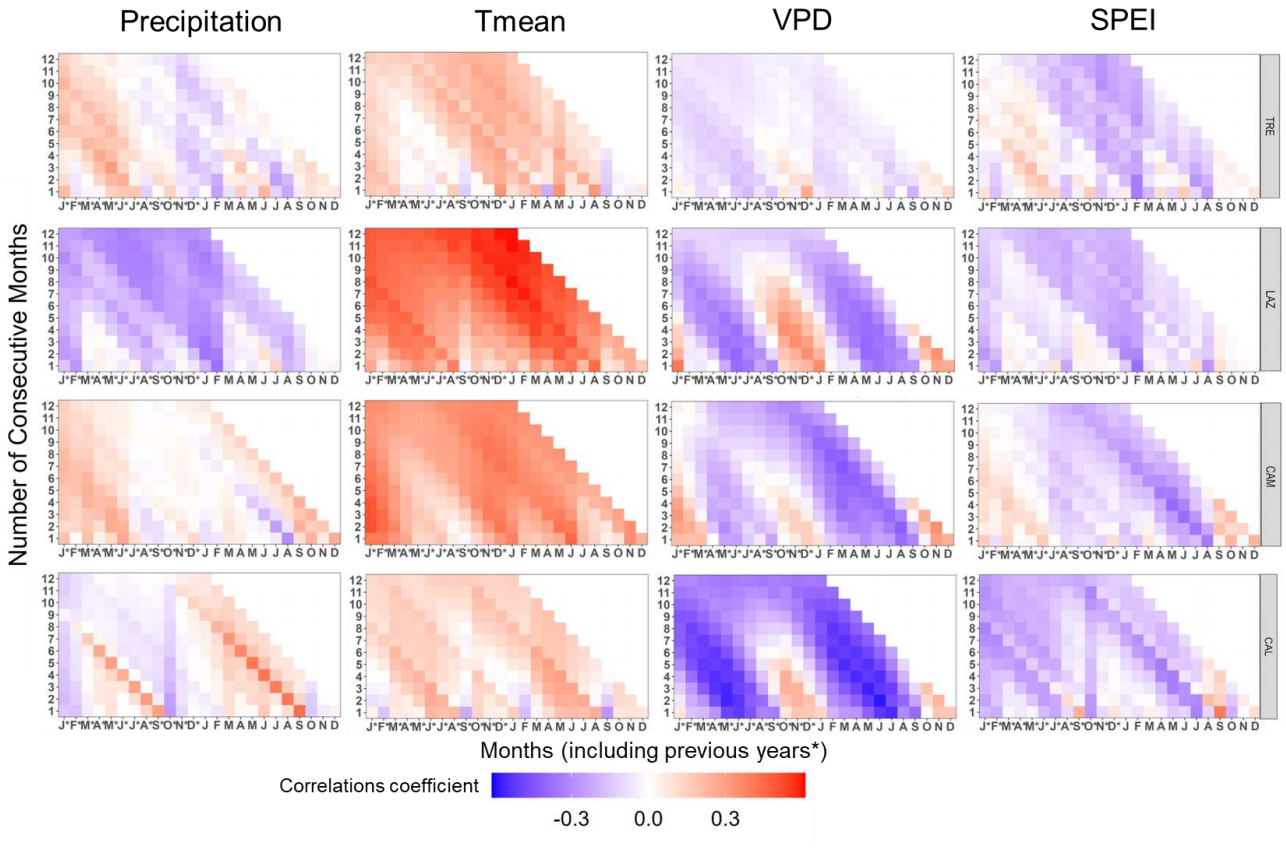

Figure 4. Pearson's running correlations between BAI with monthly precipitation, mean temperature, VPD, and SPEI1 for the current and the previous year (*) over the period 1965-2014 at each site. The *y-axis* represents the time window in months. Colours (see the key) represent correlation coefficients that are significant at the level of $r = 0.279$ ($p < 0.05$).

Growth trends of beech

The GAMMs revealed different BAI trends of beech among the four sites (Figure 5, Table S4). GAMM showed a monotonic increasing growth trend among the sites; however, they started to diverge in the mid-1990s. Notably, the northernmost site (TRE) started to decline earlier than the other sites (Figure 5). Secondly, LAZ exhibited the highest increase, followed by a drastic decline during the 2000s – a similar pattern was also observed in CAL. In contrast, the oldest site CAM trees demonstrated a steady increase in BAI over the observed period (Figure 5).

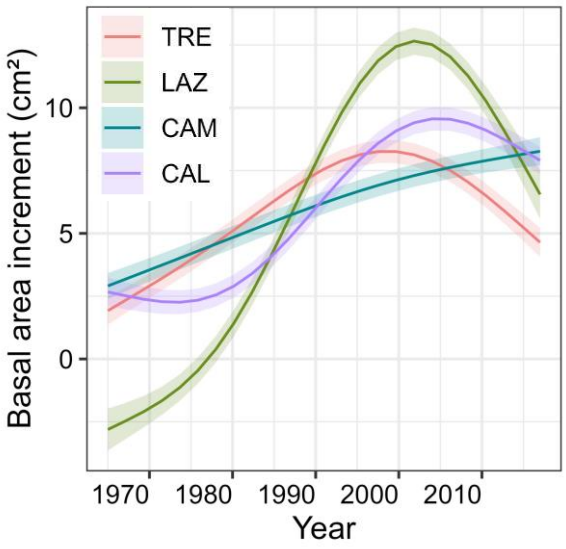

Figure 5 Growth trends of basal area increment trends of beech for the four sites. Trends were based on the best-fitted generalized additive mixed models (GAMM) for the period 1965-2014.

Long-term carbon isotope chronologies and water use strategies

At the southernmost site (CAL), trees presented the highest increase of $\delta^{13}C$ values that translate in an increase of $_{i}WUE$ (Table 3, Figure 6). On the contrary, CAM (oldest site) showed the lowest value of $_{i}WUE$ (Table 3, Figure 6). LAZ and TRE on average presented similar $\delta^{13}C$ and $_{i}WUE$ (Table 3).

Table 3. Statistics of mean $\delta^{13}C$ and $_{i}WUE$ of the tree-ring width series of beech per site for the period 1965–2014. Data are mean values ± SE.

Site	$\delta^{13}C$ (‰)	$_{i}WUE$ (µmol mol^{-1})
TRE	–25.9 ± 1.4	82.4 ± 20.4
LAZ	–25.1 ± 1.1	89.6 ± 8.7
CAM	–26.4 ± 0.9	76.9 ± 14.8
CAL	–24.8 ± 0.9	93.4 ± 13.5

For most sites, $\delta^{13}C$ showed a positive and significant trend over time ($p < 0.05$, Figure 6), except for LAZ, which showed an opposite pattern during the period 1965–2014 ($p < 0.001$, Figure 5). In the northernmost site (TRE), the $\delta^{13}C$ and $_iWUE$, started to increase sharply after the drought of 2003. Similarly, the southern sites CAM and CAL presented a steady increase in $_iWUE$ ($p < 0.001$, Figure 5). On the contrary, LAZ did not present any significant trend ($p = 0.701$).

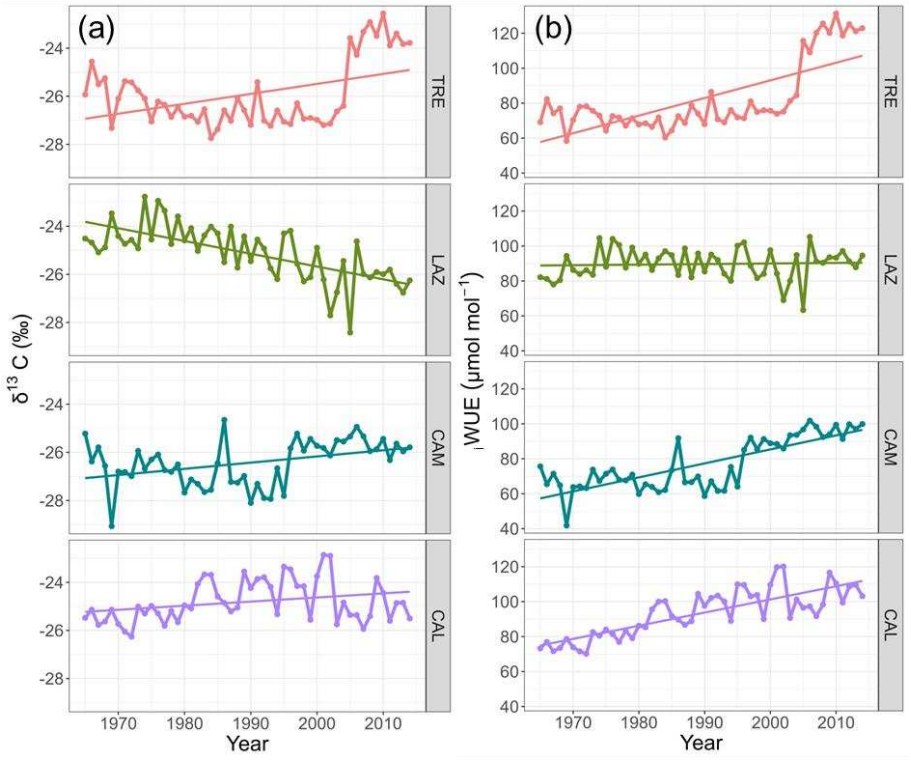

Figure 6 Trends of: a) $\delta^{13}C$ (‰), and b) $_iWUE$, and fitted linear trends for the period 1965–2014 in four stands across a latitudinal gradient in Italy.

In the southern sites, CAM and CAL, we observed significant positive relationships between $_iWUE$ and BAI ($p < 0.001$, Figure 7). On the contrary, at the northern site (TRE), we observed the opposite trend pattern; however, this trend was not significant ($p > 0.05$). AT LAZ, no relationship was found between $_iWUE$ and BAI (Figure 7).

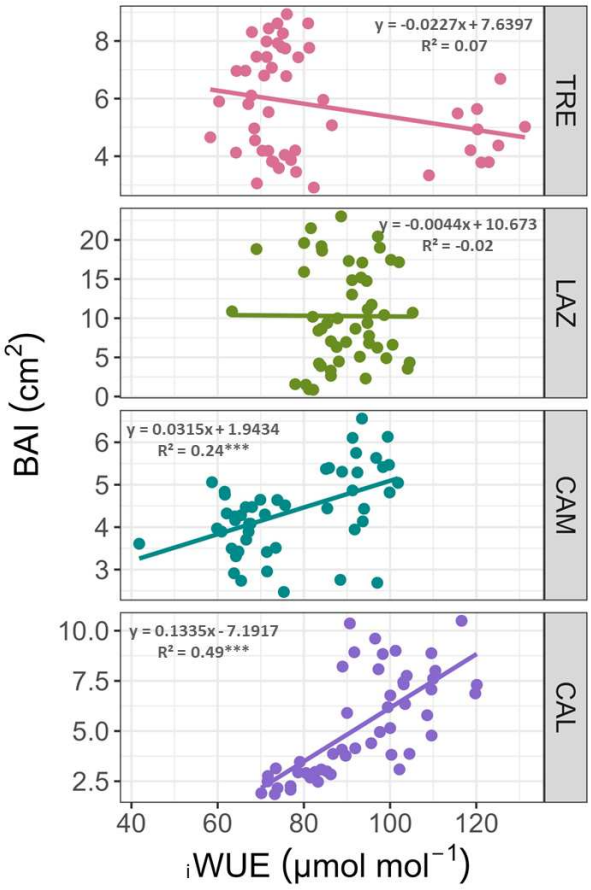

Figure 7 Relationship between annual BAI and $_{i}$WUE in beech across the Italian Peninsula for the period 1965-2014. Linear regressions and the equations are indicated for each site. Significance values are encoded by ***$p < 0.001$.

$\delta^{13}C$, *$_{i}$WUE, and climate relationship*

Carbon isotope composition ($\delta^{13}C$) and $_{i}$WUE showed a similar relationship with climate variables. However, $_{i}$WUE presented stronger correlation with climate than $\delta^{13}C$ (Figure 8, Figure S4). An exception was observed at LAZ, where $\delta^{13}C$ showed a negative and significant correlation with T_{mean} compared to $_{i}$WUE (Figure 8, Figure S4).

At the northernmost site, $_{i}$WUE showed significant and positive correlations with T_{mean} and VPD of the previous and current year, while negative and scattered correlations with P and SPEI of April and May were observed (Figure 8).

At LAZ, $_{i}$WUE was negatively and significantly correlated with VPD from March to November of the current and previous year.

At CAM, $_{i}$WUE exhibited a positive and significant correlation with P from March to May (previous and current year), while T_{mean} of the current and previous year was positively and significantly correlated with $_{i}$WUE. On the contrary, $_{i}$WUE correlated strongly and negatively with VPD from May to August (current and previous year) and with SPEI in August (Figure 8).

At the southernmost site, $_{i}$WUE correlated positively with P from March to September (current year), and strongly and positively with T_{mean} from March to August of the previous year. At CAL, VPD and SPEI exhibited strong and negative correlations with $_{i}$WUE from May to June (current and previous year, Figure 8).

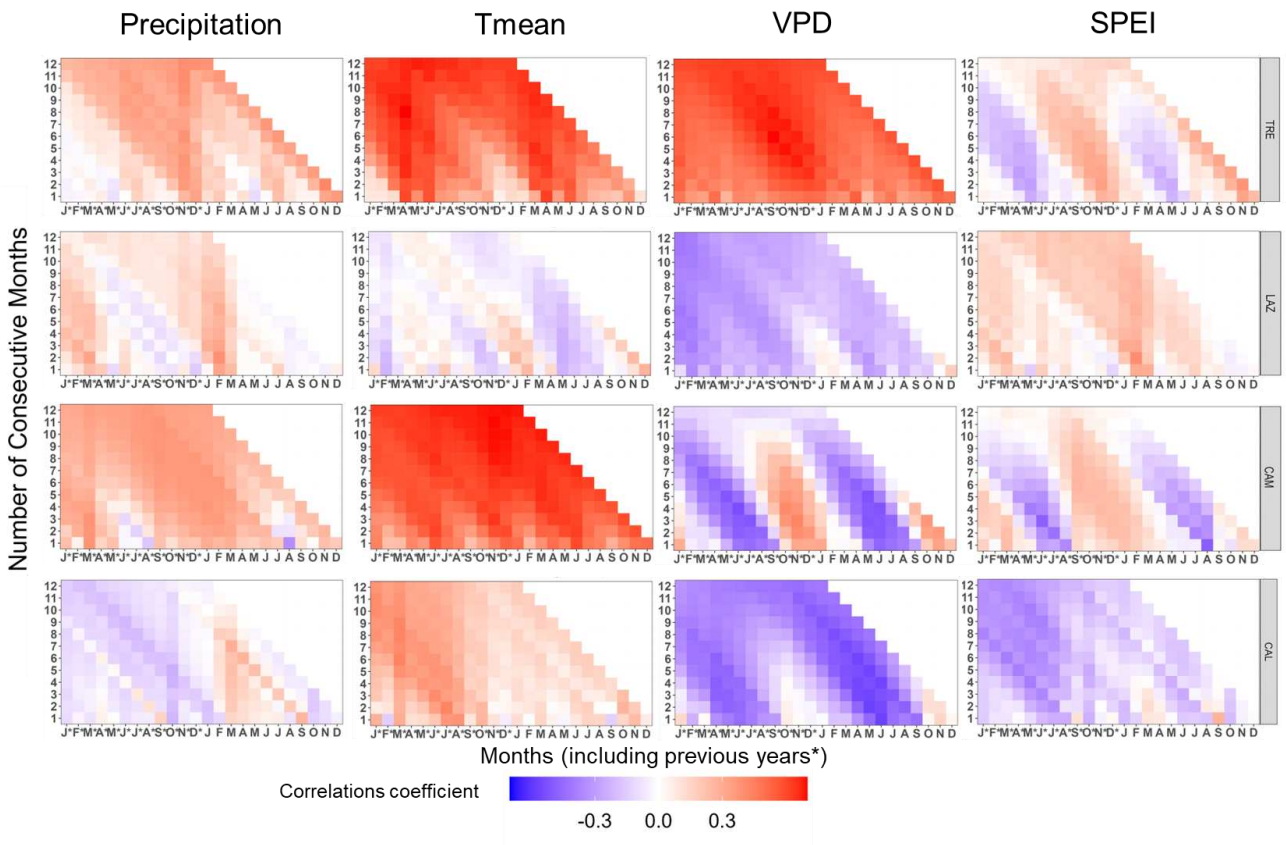

Figure 8 Pearson's running correlations between $_{i}$WUE with monthly precipitation, mean temperature, VPD, and SPEI1 for the current and the previous year (*), over the period 1965-2014 at

each site. The *y-axis* represents the time window in months. Colours (see the key) represent correlation coefficients that are significant at the level of $r = 0.279$ ($p < 0.05$)

Early warning signals of declining forest resilience

The statistical analysis of the BAI time series performed to detect EWS on beech forests revealed contrasting results among the sites (Figure 9a and 9b). In TRE and LAZ, BAI showed a rise in AR(1) among trees, which started to increase after the 2003 drought in TRE, while in LAZ already during the 1990s (Figure 9a). In contrast, CAM showed a significant steady decrease in AR(1). No significant autocorrelation trend was found at CAL, Nevertheless, the standard deviation (SD) started to rise by the end of the 1980s (Figure 9b). A significant increase in SD of the BAI signal was observed across all the sites.

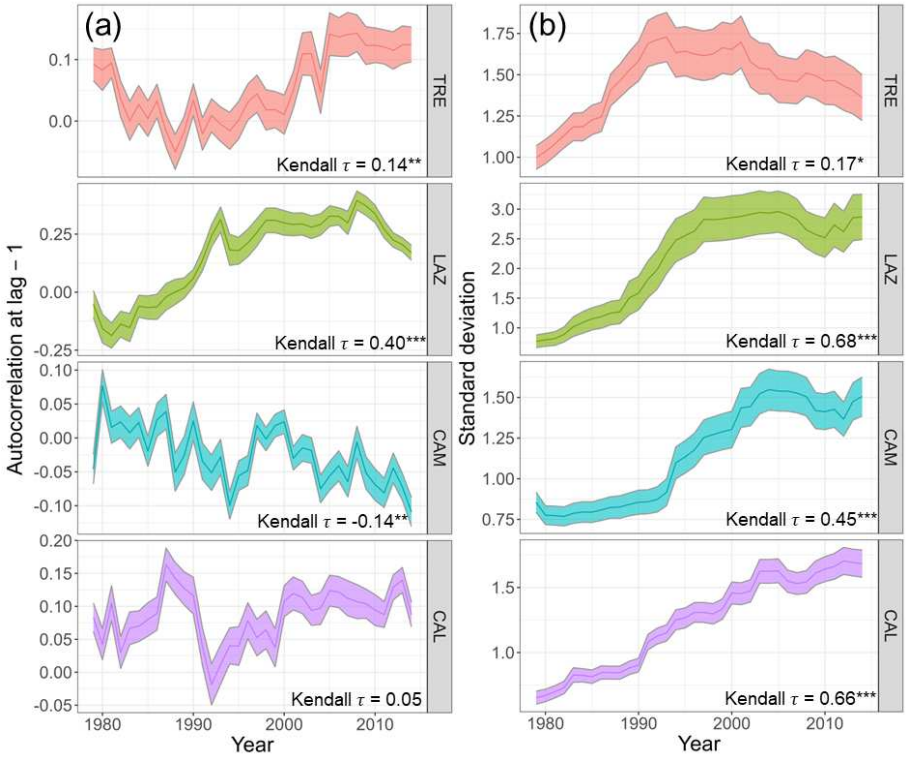

Figure 9 Early warning signals: a) AR(1), first-order autocorrelation, b) SD, obtained using a 15-year moving window for basal area increment (BAI) of *Fagus sylvatica* for four study sites for the period 1965-2014. The statistics of BAI were calculated using the residuals of the time series after

419 removing the low-frequency signal (Gaussian filter) using 15-year-long windows (e.g. 1979
420 corresponds to the interval 1965-2014). The Kendall τ statistics indicate the strength of trends along
421 the time series for each variable and site. For each site, the bold line represents the mean of the
422 statistics among trees, and the shaded area is the standard error. (* $p < 0.05$, ** $p < 0.001$, *** $p <$
423 0.001).

424

425

426 **4 DISCUSSION**

427 **Long-term growth patterns and climate variability impact on beech across Italy**

428 Our analysis revealed diverse long-term growth responses of European beech across the Italian
429 Peninsula, closely associated with local climate and site conditions. The northern sites (TRE and
430 LAZ) showed a decrease in BAI trends after the severe drought event in 2003, while the southernmost
431 site (CAL) exhibited a growth decline after 2010. In contrast, CAM displayed a steady increase in
432 growth over the 50 years analysed, likely due to increased precipitation in the last decades.

433 Our findings confirmed that European beech in the northern sites might be more susceptible to die-
434 off, even without visible decline symptoms (such as branch dieback or decolouration of leaves). Trees
435 exhibited greater growth sensitivity to VPD during summer, and this effect became more pronounced
436 at the southernmost site. VPD can be used to estimate atmospheric water status and is one of the most
437 important environmental factors influencing plant growth (Zabri and Burrage, 1997). Elevated VPD,
438 associated with dry conditions, impacts stomatal conductance and the balance between carbon
439 assimilation and water loss (McDowell et al., 2008; Zhang et al., 2015). This indicates that drought,
440 driven by enhanced evapotranspiration, will play a critical role throughout the beech forest's
441 latitudinal range in Italy.

Recent global-scale research by Yuan et al. (2019) highlighted the increase of VPD as a major atmospheric driver affecting forest productivity by imposing water stress on photosynthesis. Water-use strategies, particularly conservative/opportunistic responses within and across species, have been closely linked to soil moisture availability (Moreno-Gutiérrez et al., 2012; Martínez-Vilalta et al., 2014). Higher VPD and temperature accelerate soil moisture depletion causing a significant reduction in carbon uptake (Sulman et al., 2016), elevating the risk of drought-induced dieback through hydraulic failure and/or carbon starvation (Anderegg et al., 2016; Adams et al., 2017; Grossiord et al., 2020).

Our results demonstrate a significant increase in VPD after the 2003 drought event in TRE, however we found a weak negative correlation between VPD and BAI. We can hypothesise this might be attributed to a lower soil water holding capacity (SWHC) at this site, potentially increasing vulnerability to growth decline, as observed in our GAMM model. Conversely, LAZ exhibited higher SWHC, likely contributing to higher transpiration rates and growth compared to other sites. CAM and CAL sites presented moderate SWHC and a declining VPD trend, indicating less stress than the TRE site. The GAMM model integrated responses to the SPEI index and individual age of each tree, thus, we speculate that hydraulic strategies under drought significantly impact long-term growth rates, reflecting site-specific and ontogenic plasticity responses of the species. These findings may suggest that young beech trees initially benefit from favourable climate conditions and higher transpiration rates; however, this advantage depends on soil water availability and makes them susceptible to rapid declines in growth during extreme drought events, as already observed in Switzerland (Vanoni et al., 2016).

Our study, to our knowledge, is the first to show evidence of the negative impact of VPD on basal area increment in beech forests across the Italian peninsula. This correlation was evident in all sites but was even stronger at southern latitudes. In contrast, previous studies in mature beech stands did not find a significant climate correlation, attributed to the species' mast-seeding behaviour and

sensitivity to late frosts at the beginning of the growing season (Piovesan and Adams, 2001; Castagneri et al., 2014; D'Andrea et al., 2021; Tonelli et al., 2023). Other studies have identified lagged climate correlation with masting (Vacchiano et al., 2017). Additionally, Zimmermann et al. (2015), in central Germany, found that beech growth was highly sensitive to summer temperatures and extreme drought events after the 1980s.

Drought sensitivity and water-use strategies effect on growth

European beech has commonly been classified as an opportunistic species, capable of maintaining higher transpiration rates even in relatively dry soil conditions (Leuschner, 2020; and references therein); however, this strategy increases the risk of cavitation (McDowell et al., 2008; Martinez-Vilalta et al., 2014).

Our findings indicated that temperature and VPD emerged as primary drivers of $_{i}$WUE in TRE, while VPD played a dominant role in the southern sites. However, in LAZ, $_{i}$WUE did not exhibit a clear correlation with climate variables. This complex relationship highlights the interaction between VPD, stomatal conductance, and photosynthesis, as high VPD initially reduces stomatal conductance but not net CO_2 assimilation rate, resulting in increased $_{i}$WUE. Nevertheless, severe VPD-induced stomatal conductance restrictions, combined with declining soil moisture and other non-stomatal limitations, ultimately reduce photosynthetic rate and may lead to declining $_{i}$WUE as VPD continues to rise (Flexas et al., 2012). Thus, the overall relationship between $_{i}$WUE and VPD is likely hyperbolic (Zhang et al., 2019), and the sensitivity of photosynthesis to VPD will likely be weaker than the sensitivity of conductance to VPD.

Our study highlights contrasting water use strategies of beech across the Italian peninsula. We observed an increase of $\delta^{13}C$ and $_{i}$WUE values in TRE, CAM, and CAL, indicating a conservative water use strategy when water availability is low. In contrast, LAZ exhibited a decrease of $\delta^{13}C$,

491 suggesting an opportunistic response with stable $_i$WUE regardless of the moisture condition. While
492 at LAZ, changes in photosynthetic rate and stomatal conductance appeared to occur in the same
493 direction with similar magnitude, at TRE, CAM, and CAL, stomatal conductance appeared to
494 decrease proportionally more than photosynthetic rate, or the latter remaining stable or increasing
495 with declining stomatal conductance. Thus, our findings confirm that water use strategies employed
496 by beech are mostly site-specific and influenced by microclimatic conditions and soil water
497 availability (McCarroll and Loader, 2004), consistent with our hypothesis and consistent with prior
498 research (Peñuelas et al., 2008).

499 Interestingly, our results indicate that higher mean $_i$WUE did not result in an increase in the basal
500 area increment on beech (Nock et al., 2011; Peñuelas et al., 2011; Mazza et al., 2024); instead, we
501 observed contrasting responses consistent with previous studies (Peñuelas et al., 2008; Tognetti et al.,
502 2014). Notably, the northern site displayed a drastic increase in $_i$WUE after the 2003 drought event,
503 coinciding with elevated VPD and temperature that may have led to stomatal closure (g_s) and reduced
504 photosynthesis (A), suggesting that the growth decline in this site was might triggered by intensified
505 evapotranspiration and the lower SWHC as observed in other sites by others (e.g. Peñuelas et al.,
506 2011; Li et al., 2023). At LAZ, there was no relationship between $_i$WUE and growth, which can be
507 explained by higher SWHC allowing higher transpiration rates and metabolic respiration, resulting in
508 greater losses of photosynthetic assimilates, especially at higher temperatures (Nock et al., 2011;
509 Mazza et al., 2024). Interestingly, in the southern sites, the increase of $_i$WUE enhanced growth. This
510 discrepancy may be attributed to the adaptation of beech trees in the southernmost distribution to
511 water stress and high VPD (Anderegg et al., 2019; Battipaglia and Cherubini, 2022), suggesting that
512 high $_i$WUE is an adaptative trait (Medrano et al., 2009). Consequently, we can infer that the observed
513 "conservative strategy" - characterized by low stomatal conductance and constant CO_2 assimilation
514 rate that enhanced growth – at CAM might be explained by a positive CO_2 fertilization effect or long-
515 term acclimation to elevated CO_2 (Walker et al., 2021). Similar findings were reported in mature
516 European beech stands in Spain, where an increased sensitivity to drought was observed across the

517 southern range-edge distribution (Peñuelas et al., 2008). Recently, Qi et al. (2023) in China revealed
518 varying water use strategies among larch trees. Mature trees presented a more 'conservative strategy'
519 (low g_s, constant assimilation rate (A)), whereas young trees maintained constant g_s and high A,
520 indicating an opportunistic behaviour. Notably mature trees displayed a greater sensitivity to
521 atmospheric CO_2 concentrations than their young counterparts.

522 It should be pointed out that a major influence of photosynthetic rate on intercellular CO_2
523 concentration and $\delta^{13}C$, and the minor contribution of the regulation of stomatal conductance to
524 $_i$WUE, were observed in other studies on the same species (Tognetti et al., 2014). These findings
525 suggest unclear patterns of potential increased drought-related tree decline signs in mountain beech
526 forests along the Italian latitudinal transect. Differences between leaf-level physiology and tree-ring
527 level processes may arise, reflecting potential variations in the (re)translocation patterns of non-
528 structural carbohydrates to organs (Martínez-Vilalta et al., 2016; Merganičová et al., 2019). Such
529 complexities make tree-ring analysis a challenging tool for decipher tree responses to fluctuating
530 seasonal conditions in the short term.

531

532 **Early Warning Signals of mortality**

533 Our second hypothesis, linking the degree of growth reduction and tree growth instability to drought
534 severity, was only partially confirmed by our findings. We observed an increase in the autocorrelation
535 of the BAI signal across almost all sites, indicating heightened intrinsic biological memory of the
536 trees and signaling a loss of ecological system resilience (Lloret et al., 2011; Seidel et al., 2022; Smith
537 et al., 2022). Such increases have been linked to instabilities preceding external disturbances in
538 various biological systems (e.g., Dakos et al., 2012a; Boulton et al., 2022; Forzieri et al., 2022),
539 potentially leading to a transition to a new system state (Majumder et al., 2019; Buxton et al., 2021).
540 Recent studies investigating ecosystem productivity's autocorrelation have identified reduced
541 resilience in diverse forest types due to increased water limitations and climate variability (Forzieri

et al., 2022; Fernandez-Martinez et al., 2023). Notably, after a severe drought, declining trees exhibited increases in BAI autocorrelation and variability before mortality (Camarero et al., 2015).

In line with our expectations, the northern site showed a significant increase in AR and a decline in BAI after the 2003 drought event. Conversely, CAM showed a decrease in AR, suggesting a greater resilience to changing climate conditions, despite experiencing the severe drought period of 2003. This higher resilience at CAM might be linked to the legacy of past conditions with less water availability variability compared to the TRE site, as supported by the SPEI multiscalar index. TRE experienced several prolonged dry periods (i.e. SPEI<-1.5), before the 2000s. Additionally, the presence of relatively mature trees at CAM site might contribute to the population's apparent stability (see Colangelo et al., 2021). Our data also revealed increase BAI series SD across all stands. While this variability encompasses both tree physiological signals and climate-driven vegetation dynamics (Bochow and Boers, 2023), the co-occurrence rise in AR, decline in BAI, and increse in SD in TRE, LAZ and CAL sites, may indicate a loss of system stability (Dakos et al., 2012a). This indicates potential challenges for trees to mitigate the impact of extreme events in the future.

Several studies have demonstrated that long-term rises in instability and reduced growth predispose European beech to elevated mortality risks under future climate-induced stress conditions (Gillner et al., 2013; DeSoto et al., 2020; Cabon et al., 2023). This emphasizes the need for continuous monitoring and proactive management of beech forests, particularly in regions where climate change is projected to increase the frequency and severity of droughts. Ongoing monitoring enables early detection of tree mortality risks, facilitating timely interventions to protect and sustain these vital ecosystems with wide ecological amplitude.

5 CONCLUSIONS

In conclusion, in this study our goal was to advance the early prediction of mortality risk in healthy beech stands without, apparently, visible declining symptoms across the Italian Peninsula. This is especially pertinent considering the recent growth decline observed in this species (Piovesan et al., 2008; Martinez del Castillo et al., 2022; Dorado-Liñan et al., 2022), although the available evidence is not yet conclusive (Tognetti et al., 2014).

These findings highlight the importance of considering the plasticity and site-specific $_{i}$WUE responses to varying environmental conditions and the impact of VPD on stomatal conductance when predicting the future of beech forests in the context of climate change. It is important to note that not all beech populations considered in this study exhibited an increase in $_{i}$WUE in response to rising VPD. This variability reflects differing sensitivities to changes in environmental drivers and the plasticity of conservative to opportunistic water-use strategies.

Furthermore, our analysis of EWS reveals the loss of resilience after an extreme event, as notably observed at the TRE site. In the context of climate change projection, the increase in the frequency and severity of droughts, the ability to detect earlier tipping points of critical slow down in declining systems and the potential for recovery to the current state or an alternative state remains uncertain (Cabon et al., 2023).

Nonetheless, this research raises further questions, such as how to generalize the relationships between increased $_{i}$WUE and conservative behaviour, thus explaining contradictory results obtained in tree ring studies on beech populations and assess temporal changes in this functional trait. Further research considering young and old trees and their physiological mechanisms (Leuschner, 2020; Qi et al., 2023), micro-site conditions (Puchi et al., 2021), and genetics will also elucidate intraspecific variations in drought response (Alderotti et al., 2023). This knowledge is essential for developing effective conservation and also future forest management strategies to ensure the long-term health, vitality, and resilience of these crucial ecological and socio-economical ecosystems.

ACKNOWLEDGMENTS

P.F.P., G.B. and A.C. were supported by the MIUR project (PRIN 2020) "Unraveling interactions between WATER and carbon cycles during drought and their impact on water resources and forest and grassland ecosySTEMs in the Mediterranean climate" (WATERSTEM, cod. 20202WF53Z). E.V., and A.C were supported by the MIUR project (PRIN 2020) "Multi-scale observations to predict Forest response to pollution and climate change" (MULTIFOR, cod. 2020E52THS). P.F.P., D.D., E.V. and A.C. acknowledge funding by the project FORESTNAVIGATOR Horizon Europe research and innovation programme under grant agreement No. 101056875 and by OptForEU H2020 research and innovation programme under grant agreement No. 101060554; A.C. was also supported by resources available from the Italian Ministry of University and Research (FOE-2019), under projects 'Climate Changes' (CNR DTA. AD003.474.029). R.T. was supported by the Cost Action CA15226 - Climate-Smart Forestry in Mountain Regions (CLIMO). We also acknowledge the project funded under the National Recovery and Resilience Plan (NRRP), Mission 4 Component 2 Investment 1.4 - Call for tender No. 3138 of 16 December 2021, rectified by Decree n.3175 of 18 December 2021 of Italian Ministry of University and Research funded by the European Union – NextGenerationEU under award Number: Project code CN_00000033, Concession Decree No. 1034 of 17 June 2022 adopted by the Italian Ministry of University and Research, CUP B83C22002930006, Project title "National Biodiversity Future Centre - NBFC".

REFERENCES

Adams, H. D., Zeppel, M. J. B., Anderegg, W. R. L., Hartmann, H., Landhäusser, S. M., Tissue, D. T., Huxman, T. E., Hudson, P. J., Franz, T. E., Allen, C. D., Anderegg, L. D. L., Barron-Gafford, G. A., Beerling, D. J., Breshears, D. D., Brodribb, T. J., Bugmann, H., Cobb, R. C., Collins, A. D.,

Dickman, L. T., … McDowell, N. G. (2017). A multi-species synthesis of physiological mechanisms in drought-induced tree mortality. *Nature Ecology and Evolution*, 1(9). https://doi.org/10.1038/s41559-017-0248-x

Alderotti, F., Sillo, F., Brilli, L., Bussotti, F., Centritto, M., Ferrini, F., Gori, A., Inghes, R., Pasquini, D., Pollastrini, M., Saurer, M., Cherubini, P., Balestrini, R., & Brunetti, C. (2023). *Quercus ilex* L. dieback is genetically determined: Evidence provided by dendrochronology, $\delta^{13}C$ and SSR genotyping. *Science of The Total Environment*, 904, 166809. https://doi.org/10.1016/j.scitotenv.2023.166809

Allen, C. D., Breshears, D. D., & McDowell, N. G. (2015). On underestimation of global vulnerability to tree mortality and forest die-off from hotter drought in the Anthropocene. *Ecosphere*, 6(8), 1–55. https://doi.org/10.1890/ES15-00203.1

Allen, C. D., Macalady, A. K., Chenchouni, H., Bachelet, D., Mcdowell, N., Vennetier, M., Kitzberger, T., Rigling, A., Breshears, D. D., Hogg, E. H. (Ted) T., Gonzalez, P., Fensham, R., Zhang, Z., Castro, J., Demidova, N., Lim, J. H., Allard, G., Running, S. W., Semerci, A., & Cobb, N. (2010). A global overview of drought and heat-induced tree mortality reveals emerging climate change risks for forests. *Forest Ecology and Management*, *259*(4), 660–684. https://doi.org/10.1016/j.foreco.2009.09.001

Allen, R. G. (1993). Evaluation of a temperature difference method for computing grass reference evapotranspiration. Report submitted to FAO, Rome.

Anderegg, W. R. L., Anderegg, L. D. L., Kerr, K. L., & Trugman, A. T. (2019). Widespread drought-induced tree mortality at dry range edges indicates that climate stress exceeds species' compensating mechanisms. *Global Change Biology*, *25*(11), 3793–3802. https://doi.org/10.1111/gcb.14771

639 Anderegg, W. R. L., Klein, T., Bartlett, M., Sack, L., Pellegrini, A. F. A., Choat, B., & Jansen, S.
640 (2016). Meta-analysis reveals that hydraulic traits explain cross-species patterns of drought-
641 induced tree mortality across the globe. *Proceedings of the National Academy of Sciences of the*
642 *United States of America*, 113(18). https://doi.org/10.1073/pnas.1525678113

643 Anderegg, W. R. L., Kane, J. M., & Anderegg, L. D. L. (2013). Consequences of widespread tree
644 mortality triggered by drought and temperature stress. *Nature Climate Change*, 3(1), 30–36.
645 https://doi.org/10.1038/nclimate1635

646 Battipaglia, G., Cherubini, P. (2022). Stable Isotopes in Tree Rings of Mediterranean Forests. In:
647 Siegwolf, R.T.W., Brooks, J.R., Roden, J., Saurer, M. (eds) Stable Isotopes in Tree Rings. Tree
648 Physiology, vol 8. Springer, Cham. https://doi.org/10.1007/978-3-030-92698-4_21

649 Battipaglia, G., Pelleri, F., Lombardi, F., Altieri, S., Vitone, A., Conte, E., Tognetti, R. (2017). Effects
650 of associating *Quercus robur* L. and *Alnus cordata* Loisel. on plantation productivity and water
651 use efficiency. *Forest Ecology and Management*. 391, 106–114. https://doi.
652 org/10.1016/j.foreco.2017.02.019.

653 Beguería, S, Vicente-Serrano, S. M. (2017). Package 'SPEI'. https://cran.r-
654 project.org/web/packages/SPEI/index.html

655 Beguería, S., Vicente-Serrano, S. M., Reig, F., & Latorre, B. (2014). Standardized precipitation
656 evapotranspiration index (SPEI) revisited: Parameter fitting, evapotranspiration models, tools,
657 datasets and drought monitoring. *International Journal of Climatology*, 34, 3001–-3023.
658 https://doi.org/10.1002/joc.3887

659 Belmecheri, S., & Lavergne, A. (2020). Compiled records of atmospheric CO_2 concentrations and
660 stable carbon isotopes to reconstruct climate and derive plant ecophysiological indices from tree
661 rings. *Dendrochronologia*, 63, 125748.

662 Biondi, F., & Qeadan, F. (2008a). A theory-driven approach to tree-ring standardization: Defining
663 the biological trend from expected basal area increment. *Tree-Ring Research*, 64(2), 81–96.
664 https://doi.org/10.3959/2008-6.1

665 Biondi, F. & Qeadan, F. (2008b) Removing the tree-ring width biological trend using expected basal
666 area increment. in USDA Forest Service RMRS-P-55 124–131

667 Bochow, N., & Boers, N. (2023). The South American monsoon approaches a critical transition in
668 response to deforestation. *Science Advances*, *9*(40), eadd9973.

669 Boulton, C. A., Lenton, T. M., & Boers, N. (2022). Pronounced loss of Amazon rainforest resilience
670 since the early 2000s. *Nature Climate Change*, 12(3), 271-278.

671 Brodribb, T. J., Powers, J., Cochard, H., & Choat, B. (2020). Hanging by a thread? Forests and
672 drought. *Science*, 368(6488), 261–266. https://doi.org/10.1126/science.aat7631

673 Bunn, A., Korpela, M., Biondi, F., Campelo, F., Mérian, P., Qeadan, F., & Zang, C. (2021). dplR:
674 Dendrochronology program library in R. https://CRAN.R--proje ct.org/package=dplR

675 Bunn, A. G. (2008). A dendrochronology program library in R (dplR). *Dendrochronologia*, 26(2),
676 115–124. https://doi.org/10.1016/j.dendro.2008.01.002

677 Burnham, K.P. and Anderson, D.R. (2002). Model Selection and Inference: A Practical Information-
678 Theoretic Approach. 2nd Edition, Springer-Verlag, New York. http://dx.doi.org/10.1007/b97636

679 Buxton, J. E., Abrams, J. F., Boulton, C. A., Barlow, N., Rangel Smith, C., Van Stroud, S., ... &
680 Lenton, T. M. (2022). Quantitatively monitoring the resilience of patterned vegetation in the Sahel.
681 *Global Change Biology*, *28*(2), 571-587.

682 Cabon, A., DeRose, R. J., Shaw, J. D., & Anderegg, W. R. L. (2023). Declining tree growth resilience
683 mediates subsequent forest mortality in the US Mountain West. *Global Change Biology*, *29*(17),
684 4826–4841. https://doi.org/10.1111/gcb.16826

685 Cailleret, M., Dakos, V., Jansen, S., Robert, E. M. R., Aakala, T., Amoroso, M. M., Antos, J. A.,
686 Bigler, C., Bugmann, H., Caccianaga, M., Camarero, J. J., Cherubini, P., Coyea, M. R., Čufar, K.,
687 Das, A. J., Davi, H., Gea-Izquierdo, G., Gillner, S., Haavik, L. J., … Martínez-Vilalta, J. (2019).
688 Early-warning signals of individual tree mortality based on annual radial growth. *Frontiers in*
689 *Plant Science*, 9, 1–14. https://doi.org/10.3389/fpls.2018.01964

690 Cailleret, M., Jansen, S., Robert, E. M. R., Janda, P., Kane, J. M., Kharuk, V. I., Tognetti, R., & Jos,
691 E. (2016). A synthesis of radial growth patterns preceding tree mortality. *Global Change Biology*,
692 23, 1675–1690. https://doi.org/10.1111/gcb.13535

693 Camarero, J. J., Gazol, A., Sangüesa-Barreda, G., Oliva, J., & Vicente-Serrano, S. M. (2015). To die
694 or not to die: Early warnings of tree dieback in response to a severe drought. *Journal of Ecology*,
695 103(1). https://doi.org/10.1111/1365-2745.12295

696 Castagneri, D., Nola, P., Motta, R., & Carrer, M. (2014). Summer climate variability over the last
697 250 years differently affected tree species radial growth in a mesic Fagus-Abies-Picea old-growth
698 forest. *Forest Ecology and Management*, 320, 21–29. https://doi.org/10.1016/j.foreco.2014.02.023

699 Cherubini, P., Battipaglia, G., & Innes, J. (2021). Tree Vitality and Forest Health: Can Tree-Ring
700 Stable Isotopes Be Used as Indicators? *Current Forestry Reports,* 7, 69–80.
701 https://doi.org/https://doi.org/10.1007/s40725-021-00137-8

702 Colangelo, M., Camarero, J. J., Battipaglia, G., Borghetti, M., De Micco, V., Gentilesca, T., &
703 Ripullone, F. (2017). A multi-proxy assessment of dieback causes in a Mediterranean oak species.
704 *Tree Physiology*, 37(5), 617–631. https://doi.org/10.1093/treephys/tpx002

705 Cook, E. R & Kairiukstis, L. A. (1990). *Methods of dendrochronology*: Applications in the
706 environmental sciences. Dordrecht, Boston, MA: Kluwer Academic.

707 Gasparini, P., Di Cosmo, L., Floris, A. (2022). Area and Characteristics of Italian Forests. In:
708 Gasparini, P., Di Cosmo, L., Floris, A., De Laurentis, D. (eds) Italian National Forest Inventory—

709 Methods and Results of the Third Survey. Springer Tracts in Civil Engineering . Springer, Cham.
710 https://doi.org/10.1007/978-3-030-98678-0_7

711 Gillner, S., Rüger, N., Roloff, A., & Berger, U. (2013). Low relative growth rates predict future
712 mortality of common beech (*Fagus sylvatica* L.). *Forest Ecology and Management*, *302*, 372-378.

713 Hargreaves, G. L., Hargreaves, G. H., and Riley, J. P. (1985). Irrigation water requirements for
714 Senegal River Basin. *Journal of Irrigation and Drainage Engineering*, 111(3), 265–275.

715 Hengl, T., & Nauman, T. (2018). Predicted USDA soil great groups at 250 m (probabilities) (Version
716 v01) [Data set]. Zenodo. 10.5281/zenodo.1476844

717 Holmes, R. L. (1983). Computer-assisted quality control in tree-ring dating and measurement. *Tree-*
718 *Ring Bulletin*, 43, 69–78.

719 Dakos, V., Van Nes, E. H., D'Odorico, P., & Scheffer, M. (2012a). Robustness of variance and
720 autocorrelation as indicators of critical slowing down. *Ecology*, 93(2), 264–271.
721 https://doi.org/10.1890/11-0889.1

722 Dakos, V., Carpenter, S. R., Brock, W. A., Ellison, A. M., Guttal, V., Ives, A. R., Kéfi, S., Livina,
723 V., Seekell, D. A., van Nes, E. H., & Scheffer, M. (2012b). Methods for detecting early warnings
724 of critical transitions in time series illustrated using simulated ecological data. *PLoS ONE*, 7(7).
725 https://doi.org/10.1371/journal.pone.0041010

726 D'Andrea, E., Scartazza, A., Battistelli, A., Collalti, A., Proietti, S., Rezaie, N., Matteucci, G., &
727 Moscatello, S. (2021). Unravelling resilience mechanisms in forests: role of non-structural
728 carbohydrates in responding to extreme weather events. *Tree Physiology*, 41(10), 1808–1818.
729 https://doi.org/10.1093/treephys/tpab044

730 DeSoto, L., Cailleret, M., Sterck, F., Jansen, S., Kramer, K., Robert, E. M. R., Aakala, T., Amoroso,
731 M. M., Bigler, C., Camarero, J. J., Čufar, K., Gea-Izquierdo, G., Gillner, S., Haavik, L. J., Hereş,
732 A. M., Kane, J. M., Kharuk, V. I., Kitzberger, T., Klein, T., … Martínez-Vilalta, J. (2020). Low

733 growth resilience to drought is related to future mortality risk in trees. *Nature Communications*,
734 11(1), 1–9. https://doi.org/10.1038/s41467-020-14300-5

735 De Marco, A., Sicard, P., Feng, Z., Agathokleous, E., Alonso, R., Araminiene, V., Augustatis, A.,
736 Badea, O., Beasley, J. C., Branquinho, C., Bruckman, V. J., Collalti, A., David-Schwartz, R.,
737 Domingos, M., Du, E., Garcia Gomez, H., Hashimoto, S., Hoshika, Y., Jakovljevic, T. … Paoletti,
738 E. (2022). Strategic roadmap to assess forest vulnerability under air pollution and climate change.
739 *Global Change Biology*, 28, 5062–5085. https://doi.org/10.1111/gcb.16278

740 Dorado-Liñán, I., Ayarzagüena, B., Babst, F., Xu, G., Gil, L., Battipaglia, G., Buras, A., Čada, V.,
741 Camarero, J. J., Cavin, L., Claessens, H., Drobyshev, I., Garamszegi, B., Grabner, M., Hacket-
742 Pain, A., Hartl, C., Hevia, A., Janda, P., Jump, A. S., … Trouet, V. (2022). Jet stream position
743 explains regional anomalies in European beech forest productivity and tree growth. *Nature*
744 *Communications*, 13(1): 2015. https://doi.org/10.1038/s41467-022-29615-8

745 Fang, J., & Lechowicz, M. J. (2006). Climatic limits for the present distribution of beech (Fagus L.)
746 species in the world. *Journal of Biogeography*, 33(10), 1804–1819. https://doi.org/10.1111/j.1365-
747 2699.2006.01533.x

748 Farquhar, G. D., O'Leary, M. H., & Berry, J. A. (1982). On the relationship between carbon isotope
749 discrimination and the intercellular carbon dioxide concentration in leaves. *Australian Journal of*
750 *Plant Physiology*, 9, 121–137.

751 Farquhar, G. D., & Richards, R. A. (1984). Isotopic composition of plant carbon correlates with
752 water-use efficiency of wheat genotypes. *Australian Journal of Plant Physiology*, 11, 539–552.

753 Fernández-Martínez, M., Peñuelas, J., Chevallier, F., Ciais, P., Obersteiner, M., Rödenbeck, C., ... &
754 Janssens, I. A. (2023). Diagnosing destabilization risk in global land carbon sinks. *Nature*,
755 *615*(7954), 848-853.

Flanagan, L. B., & Farquhar, G. D. (2014). Variation in the carbon and oxygen isotope composition of plant biomass and its relationship to water-use efficiency at the leaf- and ecosystem-scales in a northern Great Plains grassland. *Plant, Cell and Environment*, 37(2), 425–438. https://doi.org/10.1111/pce.12165

Flexas, J., Barbour, M. M., Brendel, O., Cabrera, H. M., Carriquí, M., Díaz-Espejo, A., Douthe, C., Dreyer, E., Ferrio, J. P., Gago, J., Gallé, A., Galmés, J., Kodama, N., Medrano, H., Niinemets, Ü., Peguero-Pina, J. J., Pou, A., Ribas-Carbó, M., Tomás, M., … Warren, C. R. (2012). Mesophyll diffusion conductance to CO_2: An unappreciated central player in photosynthesis. *Plant Science*, 193–194, 70–84. https://doi.org/10.1016/j.plantsci.2012.05.009

Francey, R. J., Allison, C. E., Etheridge, D. M., Trundinger, C. M., Enting, I. G., Leuenberger, M., Langenfelds, R. L., Michel, E., & Steele, L. P. (1999). A 1000- year high precision record of $\delta^{13}C$ in atmospheric CO_2. Tellus B: *Chemical and Physical Meteorology*, 51(2), 170–193. https://doi.org/10.3402/tellu sb.v51i2.16269

Forzieri, G., Dakos, V., McDowell, N. G., Ramdane, A., & Cescatti, A. (2022). Emerging signals of declining forest resilience under climate change. *Nature*, 608(7923), 534–539. https://doi.org/10.1038/s41586-022-04959-9

Gagen, M., Battipaglia, G., Daux, V., et al., (2022). Climate signals in stable isotope tree-ring records. In: Siegwolf, R.T.W., Brooks, J.R., Roden, J., Saurer, M. (Eds.), Stable Isotopes in Tree Rings. Tree Physiologyvol. 8. Springer, Cham, pp. 537–579. https://doi.org/10. 1007/978-3-030-92698-4_19.

Gessler, A., Bottero, A., Marshall, J., & Arend, M. (2020). The way back: recovery of trees from drought and its implication for acclimation. *New Phytologist*, 228(6), 1704–1709. https://doi.org/10.1111/nph.16703

779 Gessler, A., Cailleret, M., Joseph, J., Schönbeck, L., Schaub, M., Lehmann, M., Treydte, K., Rigling,
780 A., Timofeeva, G., & Saurer, M. (2018). Drought induced tree mortality – a tree-ring isotope based
781 conceptual model to assess mechanisms and predispositions. *New Phytologist*, 219(2), 485–490.
782 https://doi.org/10.1111/nph.15154

783 Grossiord, C., Buckley, T. N., Cernusak, L. A., Novick, K. A., Poulter, B., Siegwolf, R. T. W., Sperry,
784 J. S., & McDowell, N. G. (2020). Plant responses to rising vapor pressure deficit. *New Phytologist*,
785 226(6), 1550–1566. https://doi.org/10.1111/nph.16485

786 Holmes, R. L. (1983). Computer-assisted quality control in tree-ring dating and measurement. *Tree-*
787 *Ring Bulletin*. https://doi.org/10.1016/j.ecoleng.2008.01.004

788 IPCC. (2021). Assessment report 6 climate change 2021: The physical science basis.
789 https://www.ipcc.ch/report/ar6/wg1/

790 Jevšenak, J., & Levanič, T. (2018). dendroTools: R package for studying linear and nonlinear
791 responses between tree-rings and daily environmental data. *Dendrochronologia*, 48, 32–39.
792 https://doi.org/10.1016/j.dendro.2018.01.005

793 Keenan, J. R. (2015). Climate change impacts and adaptation in forest management: a review. *Annals*
794 *of Forest Science*, 72, 145–167. doi: 10.1007/s13595-014-0446-5

795 Kutílek, M.., Nielsen, D.R. (1994). Soil Hydrology: Textbook for Students of Soil Science,
796 Agriculture, Forestry, Geoecology, Hydrology, Geomorphology and Other Related Disciplines;
797 Catena Verlag, Germany, pp. 370.

798 Leuschner, C. (2020). Drought response of European beech (*Fagus sylvatica* L.) A review.
799 *Perspectives in Plant Ecology, Evolution and Systematics*, 47, 125576.
800 https://doi.org/10.1016/j.ppees.2020.125576

Li, F., Xiao, J., Chen, J., Ballantyne, A., Jin, K., Li, B., Abraha, M., & John, R. (2023). Global water use efficiency saturation due to increased vapor pressure deficit. *Science*, 381(6658), 672–677. DOI: 10.1126/science.adf5041

Lloret, F., Keeling, E. G., & Sala, A. (2011). Components of tree resilience: effects of successive low-growth episodes in old ponderosa pine forests. *Oikos*, *120*(12), 1909-1920.

Majumder, S., Tamma, K., Ramaswamy, S., & Guttal, V. (2019). Inferring critical thresholds of ecosystem transitions from spatial data. *Ecology*, *100*(7), e02722.

Martinez del Castillo, E., Zang, C. S., Buras, A., Hacket-Pain, A., Esper, J., Serrano-Notivoli, R., Hartl, C., Weigel, R., Klesse, S., Resco de Dios, V., Scharnweber, T., Dorado-Liñán, I., van der Maaten-Theunissen, M., van der Maaten, E., Jump, A., Mikac, S., Banzragch, B. E., Beck, W., Cavin, L., … de Luis, M. (2022). Climate-change-driven growth decline of European beech forests. *Communications Biology*, 5(1). https://doi.org/10.1038/s42003-022-03107-3

Martínez-Vilalta, J., Poyatos, R., Aguadé, D., Retana, J., & Mencuccini, M. (2014). A new look at water transport regulation in plants. *New Phytologist*, 204(1), 105–115. https://doi.org/10.1111/nph.12912

Mazza, G., Monteverdi, M. C., Altieri, S., & Battipaglia, G. (2024). Climate-driven growth dynamics and trend reversal of *Fagus sylvatica* L. and *Quercus cerris* L. in a low-elevation beech forest in Central Italy. *Science of The Total Environment*, *908*, 168250. https://doi.org/10.1016/j.scitotenv.2023.168250

McCarroll, D., & Loader, N. J. (2004). Stable isotopes in tree rings. *Quaternary Science Reviews*, *23*(7–8), 771–801. https://doi.org/10.1016/j.quascirev.2003.06.017

McDowell, N. G., Allen, C. D., Anderson-Teixeira, K., Aukema, B. H., Bond-Lamberty, B., Chini, INL., Clark, J. S., Dietze, M., Grossiord, C., Hanbury-Brown, A., Hurtt, G. C., Jackson, R. B., Johnson, D. J., Kueppers, L., Lichstein, J. W., Ogle, K., Poulter, B., Pugh, T. A. M., Seidl, R., …

825 Xu, C. (2020). Pervasive shifts in forest dynamics in a changing world. *Science*, 368, 964.
826 https://doi.org/10.1126/science.aaz9463

827 Mcdowell, N., Pockman, W. T., Allen, C. D., Breshears, D. D., Cobb, N., Kolb, T., Plaut, J., Sperry,
828 J., West, A., Williams, D. G., Yepez, E. A., Mcdowell, N., Pockman, W. T., Allen, C. D., David,
829 D., Mcdowell, N., Cobb, N., Kolb, T., Plaut, J., & Sperry, J. (2008). Mechanisms of Plant Survival
830 and Mortality during Drought: Why Do Some Plants Survive while Others Succumb to Drought ?
831 *New Phytologist*. 178, 719–739.

832 Medrano, H., Flexas, J., Galmés, J. (2009). Variability in water use efficiency at the leaf level among
833 Mediterranean plants with different growth forms. *Plant Soil* 317(1–2):17–29.
834 https://doi.org/10.1007/s11104-008-9785-z

835 Noce, S., Collalti, A., & Santini, M. (2017). Likelihood of changes in forest species suitability,
836 distribution, and diversity under future climate: The case of Southern Europe. *Ecology and*
837 *Evolution*, *7*(22), 9358–9375. https://doi.org/10.1002/ece3.3427

838 Noce, S., Collalti, A., Valentini, R., Santinin M. (2016). Hot spot maps of forest presence in the
839 Mediterranean basin. *iForest - Biogeosciences and Forestry*, 9(5), 766–774.
840 https://doi.org/10.3832/ifor1802-009

841 Nock, C.A., Baker, P.J., Wanek, W., Leis, A., Grabner, M., Bunyavejchewin, S., Hietz, P. (2011).
842 Long-term increases in intrinsic water-use efficiency do not lead to increased stem growth in a
843 tropical monsoon forest in western Thailand. *Global Change Biology*, 17(2), 1049–1063.
844 https://doi.org/10.1111/j.1365-2486.2010.02222.x

845 Pacheco, A., Camarero, J. J., Pompa-García, M., Battipaglia, G., Voltas, J., & Carrer, M. (2020).
846 Growth, wood anatomy and stable isotopes show species--specific couplings in three Mexican
847 conifers inhabiting drought-prone areas. *Science of the Total Environment*, 698, 134055.
848 https://doi.org/10.1016/j.scito tenv.2019.134055

849 Pan, Y., Birdsey, R. A., Fang, J., Houghton, R., Kauppi, P. E., Kurz, W. A., Phillips, O. L., Shvidenko,
850 A., Canadell, S. L. L. J. G., Ciais, P., Jackson, R. B., Pacala, S. W., & Hayes, D. (2011). A Large
851 and Persistent Carbon Sink in the World's Forests. *Science*, *333*, 988–993.

852 Peñuelas, J., Canadell, J. G., & Ogaya, R. (2011). Increased water-use efficiency during the 20th
853 century did not translate into enhanced tree growth. *Global Ecology and Biogeography*, *20*(4),
854 597–608. https://doi.org/10.1111/j.1466-8238.2010.00608.x

855 Peñuelas, J., Hunt, J. M., Ogaya, R., & Jump, A. S. (2008). Twentieth century changes of tree-ring
856 $\delta^{13}C$ at the southern range-edge of *Fagus sylvatica*: Increasing water-use efficiency does not avoid
857 the growth decline induced by warming at low altitudes. *Global Change Biology*, 14(5), 1076–
858 1088. https://doi.org/10.1111/j.1365-2486.2008.01563.x

859 Petrucco, L., Nardini, A., Von Arx, G., Saurer, M., & Cherubini, P. (2017). Isotope signals and
860 anatomical features in tree rings suggest a role for hydraulic strategies in diffuse drought-induced
861 die-back of Pinus nigra. *Tree Physiology*, 37(4), 523–535. https://doi.org/10.1093/treephys/tpx031

862 Piovesan, G., Biondi, F., Di Filippo, A., Alessandrini, A., & Maugeri, M. (2008). Drought-driven
863 growth reduction in old beech (*Fagus sylvatica* L.) forests of the central Apennines, Italy. *Global*
864 *Change Biology*, 14(6), 1265–1281. https://doi.org/10.1111/j.1365-2486.2008.01570.x

865 Piovesan, G., Adams, J.M., 2001. Masting behaviour in beech: linking reproduction and climatic
866 variation. Can. J. Bot. 79, 1039–1047.

867 Puchi, P. F., Camarero, J. J., Battipaglia, G., & Carrer, M. (2021). Retrospective analysis of wood
868 anatomical traits and tree-ring isotopes suggests site-specific mechanisms triggering *Araucaria*
869 *araucana* drought-induced dieback. *Global Change Biology*, 27(25), 6394–6408.
870 https://doi.org/10.1111/gcb.15881

871 Qi, X., Cherubini, P., Treydte, K., Li, M. H., Wu, Z., He, H. S., Du, H., Fang, K., & Saurer, M. (2023).
872 Growth responses to climate warming and their physiological mechanisms differ between mature

873 and young larch trees in a boreal permafrost region. *Agricultural and Forest Meteorology*, 343:
874 109765. https://doi.org/10.1016/j.agrformet.2023.109765

875 R Core Team (2022). R: A language and environment for statistical computing. R Foundation for
876 Statistical Computing, Vienna, Austria. https://www.R-project.org/.

877 Sangüesa-Barreda, G., Camarero, J. J., Sánchez-Salguero, R., Gutiérrez, E., Linares, J. C., Génova,
878 M., Ribas, M., Tíscar, P. A., & López-Sáez, J. A. (2019). Droughts and climate warming
879 desynchronize Black pine growth across the Mediterranean Basin. *Science of the Total*
880 *Environment*, 697: 133989. https://doi.org/10.1016/j.scitotenv.2019.133989

881 Seibt, U., Rajabi, A., Griffiths, H., & Berry, J. (2008). Carbon isotopes and water use efficiency:
882 Sense and sensitivity. *Oecologia*, 155, 441–454. https://doi.org/10.1007/s0044 2-007-0932-7

883 Seidl, R., Jentsch, A., & Wohlgemuth, T. (2022). Disturbance Resilience. In *Disturbance Ecology*
884 (pp. 97-115). Cham: Springer International Publishing.

885 Smith, T., Traxl, D., & Boers, N. (2022). Empirical evidence for recent global shifts in vegetation
886 resilience. *Nature Climate Change*, *12*(5), 477-484.

887 Sulman, B. N., Roman, D. T., Yi, K., Wang, L., Phillips, R. P., & Novick, K. A. (2016). High
888 atmospheric demand for water can limit forest carbon uptake and transpiration as severely as dry
889 soil. *Geophysical Research Letters*, *43*(18), 9686–9695. https://doi.org/10.1002/2016GL069416

890 Stokes, M. A., & Smiley, T. L. (1968). An introduction to tree-ring dating. Chicago, IL: University
891 of Chicago Press

892 Timofeeva, G., Treydte, K., Bugmann, H., Rigling, A., Schaub, M., Siegwolf, R., & Saurer, M.
893 (2017). Long-term effects of drought on tree-ring growth and carbon isotope variability in Scots
894 pine in a dry environment. *Tree Physiology*, 37(8), 1028–1041.
895 https://doi.org/10.1093/treephys/tpx041

Tetens, O. (1930). Uber einige meteorologische Begriffe Z. Geophys. 6, 297–309.

Title, P. O., & Bemmels, J. B. (2018). ENVIREM: an expanded set of bioclimatic and topographic variables increases flexibility and improves performance of ecological niche modeling. *Ecography*, 41(2), 291–307. https://doi.org/10.1111/ecog.02880

Tognetti, R., Lombardi, F., Lasserre, B., Cherubini, P., & Marchetti, M. (2014). Tree-ring stable isotopes reveal twentieth-century increases in water-use efficiency of *fagus sylvatica* and *nothofagus* spp. in Italian and Chilean Mountains. *PLoS ONE*, *9*(11). https://doi.org/10.1371/journal.pone.0113136

Tonelli, E., Vitali, A., Malandra, F., Camarero, J. J., Colangelo, M., Nolè, A., Ripullone, F., Carrer, M., & Urbinati, C. (2023). Tree-ring and remote sensing analyses uncover the role played by elevation on European beech sensitivity to late spring frost. *Science of the Total Environment*, 857. https://doi.org/10.1016/j.scitotenv.2022.159239

Trugman, A. T., Anderegg, L. D. L., Anderegg, W. R. L., Das, A. J., & Stephenson, N. L. (2021). Why is tree drought mortality so hard to predict? *Trends in Ecology and Evolution*, 36(6), 520–-532. https://doi. org/10.1016/j.tree.2021.02.001

Vacchiano, G., Hacket-Pain, A., Turco, M., Motta, R., Maringer, J., Conedera, M., Drobyshev, I., & Ascoli, D. (2017). Spatial patterns and broad-scale weather cues of beech mast seeding in Europe. *New Phytologist*, *215*(2), 595–608. https://doi.org/10.1111/nph.14600

Vanoni, M., Bugmann, H., Nötzli, M., & Bigler, C. (2016). Quantifying the effects of drought on abrupt growth decreases of major tree species in Switzerland. *Ecology and Evolution*, 6(11), 3555–3570. https://doi.org/10.1002/ece3.2146

Versace, S., Gianelle, D., Garfì, V., Battipaglia, G., Lombardi, F., Marchetti, M., & Tognetti, R. (2020). Interannual radial growth sensitivity to climatic variations and extreme events in mixed-

919 species and pure forest stands of silver fir and European beech in the Italian Peninsula. European
920 *Journal of Forest Research*, 139(4), 627–645. https://doi.org/10.1007/s10342-020-01274-8

921 Vicente--Serrano, S. M., Beguería, S., & López-Moreno, J. I. (2010). A Multi-scalar drought index
922 sensitive to global warming: The Standardized Precipitation Evapotranspiration Index - SPEI.
923 *Journal of Climate*, 23, 1696–1718. https://doi.org/10.1175/2009J CLI29 09.1

924 Walker, A. P., De Kauwe, M. G., Bastos, A., Belmecheri, S., Georgiou, K., Keeling, R. F., McMahon,
925 S. M., Medlyn, B. E., Moore, D. J. P., Norby, R. J., Zaehle, S., Anderson-Teixeira, K. J.,
926 Battipaglia, G., Brienen, R. J. W., Cabugao, K. G., Cailleret, M., Campbell, E., Canadell, J. G.,
927 Ciais, P., … Zuidema, P. A. (2021). Integrating the evidence for a terrestrial carbon sink caused
928 by increasing atmospheric CO2. *New Phytologist*, *229*(5), 2413–2445.
929 https://doi.org/10.1111/nph.16866

930 Walthert, L., Ganthaler, A., Mayr, S., Saurer, M., Waldner, P., Walser, M., Zweifel, R., & von Arx,
931 G. (2021). From the comfort zone to crown dieback: Sequence of physiological stress thresholds
932 in mature European beech trees across progressive drought. *Science of the Total Environment*, *753*.
933 https://doi.org/10.1016/j.scitotenv.2020.141792

934 Willmott, C. J., & Feddema, J. J. (1992). A More Rational Climatic Moisture Index*. *The*
935 *Professional Geographer*, *44*(1), 84-88. https://doi.org/10.1111/j.0033-0124.1992.00084.x

936 Wood, S. N. (2006). Low--rank scale--invariant tensor product smooths for generalized additive
937 mixed models. Biometrics, 62(4), 1025–-1036. https://doi.org/10.1111/j.1541-
938 -0420.2006.00574.x

939 Yuan, W., Zheng, Y., Piao, S., Ciais, P., Lombardozzi, D., Wang, Y., Ryu, Y., Chen, G., Dong, W.,
940 Hu, Z., Jain, A. K., Jiang, C., Kato, E., Li, S., Lienert, S., Liu, S., Nabel, J. E. M. S., Qin, Z., Quine,
941 T., … Yang, S. (2019). Increased atmospheric vapor pressure deficit reduces global vegetation
942 growth. *Science Advances*, 5(8), 1–13. https://doi.org/10.1126/sciadv.aax1396

943 Zabri, A.W. and Burrage, S.W. (1997). THE EFFECTS OF VAPOUR PRESSURE DEFICIT (VPD) AND
944 ENRICHMENT WITH CO2 ON WATER RELATIONS, PHOTOSYNTHESIS, STOMATAL
945 CONDUCTANCE AND PLANT GROWTH OF SWEET PEPPER (*CAPSICUM ANNUM* L.) GROWN
946 BY NFT. Acta Horticulturae, 449, 561–568. https://doi.org/10.17660/ActaHortic.1997.449.78

947 Zhang, Q., Ficklin, D. L., Manzoni, S., Wang, L., Way, D., Phillips, R. P., & Novick, K. A. (2019).
948 Response of ecosystem intrinsic water use efficiency and gross primary productivity to rising
949 vapor pressure deficit. *Environmental Research Letters*, 14: 074023. https://doi.org/10.1088/1748-
950 9326/ab2603

951 Zhang, K., Kimball, J. S., Nemani, R. R., Running, S. W., Hong, Y., Gourley, J. J., & Yu, Z. (2015).
952 Vegetation Greening and Climate Change Promote Multidecadal Rises of Global Land
953 Evapotranspiration. *Scientific Reports*, 5:15956. https://doi.org/10.1038/srep15956

954 Zimmermann, J., Hauck, M., Dulamsuren, C., & Leuschner, C. (2015). Climate Warming-Related
955 Growth Decline Affects Fagus sylvatica, But Not Other Broad-Leaved Tree Species in Central
956 European Mixed Forests. *Ecosystems*, 18(4), 560–572. https://doi.org/10.1007/s10021-015-9849-
957 x

958 Zuidema, P. A., Poulter, B., & Frank, D. C. (2018). A Wood Biology Agenda to Support Global
959 Vegetation Modelling. *Trends in Plant Science*, *23*(11), 1006–1015.
960 https://doi.org/10.1016/j.tplants.2018.08.003